23-12-2005

Measurements of Trace Gas Emissions from Australian Forest Fires and Correlations with Coincident Measurements of Aerosol Optical Depth

Clare Paton-Walsh
University of Wollongong, clarem@uow.edu.au

N. B. Jones
University of Wollongong, njones@uow.edu.au

Stephen R. Wilson
University of Wollongong, swilson@uow.edu.au

V Haverd
University of Wollongong, vanessah@uow.edu.au

A. Meier
University of Wollongong

See next page for additional authors

Measurements of Trace Gas Emissions from Australian Forest Fires and Correlations with Coincident Measurements of Aerosol Optical Depth

Abstract

We present vertically integrated measurements of C2H2, C2H4, C2H6, HCOOH, CO, H2CO, HCN and NH3 through smoke plumes from Australian forest fires measured by ground-based solar absorption spectroscopy. The column amounts of these gases are highly correlated with simultaneous, co-located measurements of aerosol optical depth, providing a potential method of mapping biomass-burning emissions using satellite measurements of aerosol optical depth. We have calculated emission ratios relative to CO for the trace gases using aerosol optical depth as a proxy for CO and converted to emission factors by using an average emission factor for CO from literature measurements of extra-tropical forest fires. The results show that Australian forest fire emissions are broadly similar to those from other geographical regions except for comparatively low emissions of C2H6.

Keywords

GeoQUEST

Disciplines

Life Sciences | Physical Sciences and Mathematics | Social and Behavioral Sciences

Publication Details

An edited version of this paper was published by the American Geophysical Uniion as Paton-Walsh, C, Jones, NB, Wilson, SR, Haverd, V, Meier, A and Griffith, DWT, Measurements of Trace Gas Emissions from Australian Forest Fires and Correlations with Coincident Measurements of Aerosol Optical Depth, Journal of Geophysical Research - Atmospheres, 110, 23 December 2005, D24. Copyright 2005 American Geophysical Union. Original article available here.

Authors

Clare Paton-Walsh, N. B. Jones, Stephen R. Wilson, V Haverd, A. Meier, and D. W. Griffith

Measurements of Trace gas Emissions from Australian Forest Fires and Correlations with Coincident Measurements of Aerosol Optical Depth

Clare Paton-Walsh, Nicholas B. Jones, Stephen R. Wilson, Vanessa Haverd, Arndt Meier, and David W. T. Griffith

Department of Chemistry, University of Wollongong, Australia.

Curtis P. Rinsland

NASA Langley Research Center, Mail Stop 401A, Hampton, VA 23681-2199, U.S.A

Abstract

We present vertically integrated measurements of C_2H_2, C_2H_4, C_2H_6, HCOOH, CO, H_2CO, HCN and NH_3 through smoke plumes from Australian forest fires measured by ground-based solar absorption spectroscopy. The column amounts of these gases are highly correlated with simultaneous, co-located measurements of aerosol optical depth, providing a potential method of mapping biomass-burning emissions using satellite measurements of aerosol optical depth. We have calculated emission ratios relative to CO for the trace gases using aerosol optical depth as a proxy for CO and converted to emission factors by using an average emission factor for CO from literature measurements of extra-tropical forest fires. The results show that Australian forest fire emissions are broadly similar to those from other geographical regions except for comparatively low emissions of C_2H_6.

1. Introduction

Biomass burning releases large amounts of trace gases and particulates into the atmosphere, significantly affecting global atmospheric chemistry, degrading air quality, and impacting on radiative transfer in the atmosphere [*Crutzen and Andreae*, 1990]. In the last two decades there has been significant effort to characterise fire emissions around the globe with many large-scale ground-based and airborne measurement campaigns of biomass burning [*Delmas et al.*, 1999; *Fishman et al.*, 1996; *Kaufman and al*, 1998; *Lacaux et al.*, 1995; *Lindesay et al.*, 1996; *Swap et al.*, 2003; *Torres et al.*, 2005]. The resulting body of information on the emission characteristics of different types of biomass fires in savannas and grasslands, tropical and extra-tropical forests, bio-fuel consumption, charcoal burning and agricultural residue burning have been collated and summarised recently [*Andreae and Merlet*, 2001]. Where multiple measurements exist the scatter in results is often large, not only because of real variability in emissions from different fires, but also because of the difficulty of obtaining a good representative average sample of the smoke plume. This is made especially problematic by the significantly different emissions that result from smouldering and flaming combustion stages in a single fire. Ground-based sampling tends to over-represent smouldering emissions which are typically emitted during less vigorous burning stages and hence tend to remain closer to the ground. In contrast flaming combustion emissions are lofted to higher altitudes due to hotter burning conditions and so airborne measurements may be biased towards these emissions.

This study describes vertically integrated measurements made by ground-based spectrometers using the sun as a source and extends the work reported previously [*Paton-Walsh et al.*, 2004]. Measurements were made on more than thirty separate days, through smoke plumes originating from bushfires only a few kilometres away to distant bushfires

hundreds of kilometres away. These measurements constitute a varied sample, which we believe is representative of typical Australian temperate forest fires.

2. Measurements

During the 2001/2002 and 2002/2003 austral summers, we recorded more than one thousand infrared solar atmospheric absorption spectra at Wollongong NSW, Australia (34.5°S, 150°E, 20m above sea level) through smoke plumes originating from many different bush-fires. Simultaneous and co-located direct solar spectral irradiance measurements spanning the ultra-violet and visible wavelengths were made every 20-30 seconds, using an Ocean Optics OD2000 grating spectrometer with a 2048 pixel CCD detector array, so that the optical depth of the atmosphere during the time of the infrared measurements could be determined. The infrared solar atmospheric absorption spectra were recorded using a Bomem DA8 high-resolution Fourier transform infrared spectrometer coupled to a solar tracker that transmits the direct solar beam to the entrance aperture of the spectrometer. The tracker has both active and passive tracking systems and is able to follow the sun through smoke plumes that are essentially opaque in the visible. Spectra were recorded in seven separate regions of the infrared from 700 cm^{-1} to 4500 cm^{-1} using Mercury Cadmium Telluride and Indium Antimonide detectors, and a series of seven different IR band pass filters [*Griffith et al.*, 1998]. Typical measurement times per spectra ranged from 3 to 15 minutes depending on the optical path difference employed (50 to 250 cm).

3. Analysis

3.1 Analysis of Visible Spectra for Aerosol Optical Depth

The spectral irradiance measurements were calibrated using the Langley technique to derive the top of the atmosphere signal from data collected on clear days before and after the smoke measurements [*Wilson and Forgan*, 2002]. Individual estimates of aerosol optical depth (AOD) at 500 nm were derived from each measurement of directly transmitted light through subtraction of the Rayleigh scattering component, and the mean value calculated for the period of time taken to record each of the infrared spectra. Although our measurements span the visible spectrum, maximum signal intensity and minimum interference by molecular absorbance is obtained at 500nm. Elevated AOD values can result from cloud cover as well as smoke, however since cloud strongly attenuates the mid-infrared signal, the strength of the infrared signal has allowed periods of significant cloud interference to be removed from the measurement dataset. By using a combination of elevated AOD values and attenuated infrared signal, all data (both UV/visible and IR), are successfully screened for clouds.

3.2 Analysis of Infrared Spectra for Trace Gas Amounts

The number of molecules per square centimetre of each trace gas above the measurement site (the vertical column amount) was derived from individual spectra in the appropriate filter regions by iteratively adjusting the concentration of the target gas in a simulated spectral interval (or intervals) until the difference between measured and simulated spectrum was minimised. The simulated spectrum used a layered model of the atmosphere, with the pressure, temperature and an initial concentration for each gas assigned over 39 layers. Retrievals were performed using the SFIT2 non-linear iterative fitting algorithm [*Rinsland et al.*, 1998], which is based on Rodgers optimal estimation method [*Rodgers*, 2000] returning

the concentration profile of the target gas which best fits a suitably weighted combination of the measured and simulated spectra. The *a priori* profile of the simulated spectrum is weighted by the covariance matrix (a matrix that defines the expected variation in the concentration of the target gas at each layer of the simulation). The measured spectrum is weighted by an empirically defined matrix with diagonal elements defined by the signal-to-noise ratio in the spectral interval of interest, and off-diagonal elements defined by a Gaussian function with an assumed interlayer correlation length of 4km.

The study described here includes both the first analysis of the smoke-affected atmospheric absorption spectra for acetylene (C_2H_2), ethylene (C_2H_4), ethane (C_2H_6) and formic acid (HCOOH) and reanalysis of the spectra for carbon monoxide (CO), hydrogen cyanide (HCN), formaldehyde (H_2CO) and ammonia (NH_3) previously reported [*Paton-Walsh et al.*, 2004]. This work expands on the recent study of C_2H_4 for a particular fire scene by [*Rinsland et al.*, 2005] that using selected Wollongong smoke affected spectra from a single day. The initial analysis used monthly average pressure and temperature profiles and *a priori* concentration profiles typical of clean air conditions with the analysis weighted to allow very large variability in the boundary layer and lower troposphere to achieve a good fit. In this study daily temperature and pressure data from balloon sondes launched from Sydney airport (80km to the North) were splined with National Centers for Environmental Prediction data to give more accurate temperature and pressure profiles. *A priori* concentration profiles typical of Northern Hemisphere clean air were used for the initial analysis, but this was followed by a second stage of analysis that used the average of the retrieved profiles from the initial analysis as the new *a priori* concentration profile and the variance of the concentration at each altitude layer as the basis on which to construct a new covariance matrix. For several gases (C_2H_4, HCOOH, HCN, H_2CO and NH_3), the variance of the first stage retrievals was

similar to that of carbon monoxide and a single covariance matrix was used in all these cases. Also the analysis of HCOOH and C_2H_4 used a single retrieval stage with an a priori concentration typical of clean air because using the average retrieved profile produced instabilities in the retrievals. In addition, a more thorough uncertainty analysis has been undertaken and for reasons of consistency and completeness, the reanalyses of CO, HCN, H_2CO and NH_3 are presented here alongside those of the new trace gases. Table 1 shows the spectral interval or intervals used for the retrieval of each trace gas, the interfering gases that were also fitted in the retrieval, and the mean values of the main uncertainties affecting the precision of these retrievals.

3.3 Uncertainty Analysis

The effects of pressure broadening on the shapes of absorption features allow for limited vertical resolution in the measurements. The smoothing uncertainty is the uncertainty in the total column amount that results from the inability of the retrieval to distinguish perfectly between absorption at different altitudes [*Rodgers*, 2000]. The signal-to-noise uncertainty is the column amount of each trace gas that would produce the equivalent area of absorption feature as the noise in each spectrum. This uncertainty is the dominant uncertainty for many of our target gases because of the small absorption features being fitted. These first two uncertainties were calculated separately for each individual spectrum, and the values given in Table 1 are the mean of all spectra. Also included are the temperature sensitivities of the absorption features used, multiplied by a temperature uncertainty of 5°C. The temperature uncertainty was derived from variability in balloon sonde measurements over a 12 to 24 hour time period at the height of the smoke plumes. This uncertainty in temperature is quite large because of the large temperature variations in the boundary layer and lower troposphere where the majority of the target gases are concentrated. Finally these three independent

components of uncertainty are added in quadrature to give a total uncertainty for each spectrum. Note that the total uncertainty is calculated for each individual spectrum by summing in quadrature the contributing uncertainties for that particular spectrum. The mean total uncertainty that results differs slightly from the sum in quadrature of the mean of the contributing uncertainties for all spectra.

4. Correlations between Aerosol Optical Depth and Column Amounts of Trace Gases

Figures 1 (a)-(h) show vertical column amounts of CO, H_2CO, C_2H_6, HCN, C_2H_4, NH_3, HCOOH and C_2H_2 plotted against simultaneous, co-located measurements of AOD. The data have been colour-coded to distinguish different measurement time periods. The error-bars are the total uncertainty for each spectrum calculated as described above and the one sigma standard deviation of the aerosol optical depth measurements during the time taken to record each infrared spectrum. The correlations between the trace gases and AOD, evident from the plots, are consistent for hundreds of independent spectra from many different fire episodes over all the different time-periods with the exception of the spectra recorded on January 1, 2002. On the morning of January 1, 2002 there was thick smoke trapped near ground level and four spectra were recorded before the arrival of a distinctive smoke plume was noted. These four spectra used the optical filters that transmitted in the regions used to derive C_2H_4, NH_3 and HCOOH, and both of the regions used to derive CO. By comparison with this January 1 morning data and other days, it appears that the AOD is low rather than other gases being high. After the arrival of this plume most of the plots show exceptional behaviour, with much higher trace gas to AOD ratios. A possible explanation for this anomalous data is that the smoke plume sampled on January 1, 2002 was from one of the fires burning very near the measurement site (< 5km) and the aerosols had not yet coalesced into a comparably stable

form, resulting in a lower AOD value than normal. For this reason the data from January 1, 2002 have been excluded from the regression analysis.

The gases shown in Figure 1 are all highly correlated with AOD. These correlations are significant because of their potential use in tracking biomass-burning plumes from satellites. Table 2 shows the results of generalised least squares orthogonal distance regression analysis (http://www.eurometros.org/ Distributions: "xgenline") on the column amounts of each trace gas and the coincident AOD measurements. The regression equations relating AOD to these trace gases may be used to translate a satellite measurement of AOD into an estimated column amount of each trace gas present in a fire-affected region (see [*Paton-Walsh et al.*, 2004]). This can be used to map biomass-burning emissions from satellites and better constrain chemical transport models to get more accurate estimates of total emissions from fire episodes. These measurements are representative of Australian forest fires only; no data for fires in other regions of the world have been analysed using this method.

5. Emission ratios of trace gases using Aerosol Optical Depth as a proxy for carbon monoxide

Trace gas concentrations within smoke plumes can vary rapidly with time, so the concentration levels are usually converted to relative emission ratios by dividing by coincident measurements of CO or CO_2 [*Hurst et al.*, 1994a]. Our chosen reference gas is CO, because the excess levels of CO_2 present in smoke are difficult to measure with sufficient accuracy against its large and variable background amount. In this study we have no coincident measurements of CO with the other trace gases because the column amounts are derived from spectra recorded at different times using different optical filters. Depending on filter combinations, the difference in times between various tracers and CO could be

between 10 and 30 minutes. Instead we have calculated molar emission ratios with respect to CO using AOD as a *de-facto* measurement of the CO column via the regression equation given in Table 2.

First, all data with AOD less than 1.0 were excluded because of the large uncertainties introduced when taking the ratio of two small numbers. For the remaining spectra, we calculated emission ratios by dividing the excess amount of the trace gas over background levels by the excess amount of CO over background levels. The choice of background aerosol optical depth is not critical for this analysis as it is very low. We have chosen a background optical depth of 0.03, based on analysis of earlier measurements at Wollongong [*Phillips*, 2001] and the long-term aerosol optical depth record observed at Cape Grim [*Wilson and Forgan*, 2002]. The background values for CO and the other tracers where obtained from the intercept of the regression plots with respect to AOD (see Table 2). The resulting emission ratios are given in Table 3.

6. Emission Factors Extrapolated from Emission Ratios to CO

A parameter frequently used to characterise emissions from fires is the emission factor, which is defined as the amount of a compound released per amount of dry fuel consumed, expressed in units of g kg^{-1}. To convert our data from emission ratios with respect to CO to emission factors, we use the following equation:

$$\mathbf{EF_X = ER_{(X/CO)}.(MW_X/MW_{CO}).EF_{CO}}$$

(where EF_X = the emission factor for trace gas X; $ER_{(X/CO)}$ = the molar emission ratio of trace gas with respect to CO; MW_X = the molecular weight of trace gas X; MW_{CO} = the

molecular weight of CO and EF_{CO} = the emission factor for CO [Andreae and Merlet, 2001]).

The emission ratios from this study have been converted to emission factors using the mean emission factor for CO, (EF_{CO}) for extra-tropical forests of 107 ± 37 g kg^{-1} (personal communication, M.O. Andreae, 2005. An update of previous estimates [*Andreae and Merlet*, 2001]). These emission factors are given in Table 3 alongside the mean emission factor of each trace gas from extra-tropical forest measurements taken from [*Andreae and Merlet*, 2001]. The uncertainties quoted for this study are derived from the large uncertainty in the emission factor for CO, (35%), combined in quadrature with the one-sigma standard deviation in the emission ratio to CO for each trace gas. The uncertainties shown for the mean emission factors from extra-tropical forest measurements are the one-sigma standard deviations of all the measurements used. Note that the literature based emission factor for HCN, given in parenthesis, is an estimate extrapolated from measurements from savannah fires.

The emission factors calculated for Australian temperate forest fires in this study for C_2H_2, HCOOH and H_2CO agree well with the average for all extra-tropical forests, while those for C_2H_4 and NH_3 are comparatively low, but lie within one-sigma uncertainties levels. Most of our measurements occur many kilometres downwind of the fires and so shorter-lived species may yield lower than the expected emission ratios with respect to CO. The age of smoke sampled in our dataset varies between different time periods and this contributes to the variability of the shorter-lived species. Only our results for the emission factors of HCN and C_2H_6 show significant departure from the values quoted by Andreae and Merlet. In the case of HCN the Andreae and Merlet value is questionable because it is a “best guess”, (based on

an extrapolation from measurements made from savannah and grassland fires), whilst our value for HCN of (0.43 ± 0.22) g kg^{-1} is in better agreement with airborne FTIR measurements through smoke plumes from Alaskan forest fires of 0.61 g kg^{-1} [*Goode et al.*, 2000].

For C_2H_6, our measurement uncertainties are low; the expected atmospheric lifetimes of CO and C_2H_6 are similar [*Trentmann et al.*, 2003] and hence the emission ratio with respect to CO is very consistent throughout our measurements from many different fire episodes. We note that previously reported emission ratios for C_2H_6 from Northern Australian savannah fires by Shirai *et al.* [2003] are consistent with those reported here but lower than those reported by Hurst *et al.* [1994b]. The high range data of Hurst *et al.* [1994b] used a limited number of grab samples that may not have been well mixed enough to provide a truely representative sample. We conclude that relatively low emission of C_2H_6 is a characteristic of Australian temperate forest fires where the fuel source is predominantly varieties of Eucalyptus trees.

7. Conclusions

A thorough analysis of ground-based solar absorption spectra taken through smoke plumes from Australian forest fires has yielded vertically integrated measurements of C_2H_2, C_2H_4, C_2H_6, HCOOH, CO, H_2CO, HCN and NH_3 emissions. The emissions measurements are well correlated with simultaneous, co-located measurements of aerosol optical depth, suggesting a potential use of satellite-based AOD measurements in tracking the gaseous emissions from biomass burning. This possibility is made especially interesting because satellite-based AOD measurements are sensitive right down to ground-level [*Gonzalez et al.*, 2003], unlike most satellite-based measurements of trace gases.

Emission ratios with respect to carbon monoxide have been calculated for C_2H_2, C_2H_4, C_2H_6, HCOOH, H_2CO, HCN and NH_3 using aerosol optical depth as a proxy for CO. Converting to emission factors using an average value for the emission factor of CO from previous studies indicates that Australian forest fire emissions are broadly similar to those from other geographical regions except for comparatively low emissions of C_2H_6.

Acknowledgements

We thank the Australian Research Council for its support of this work and the Atmosphere Watch Section of the Australian Bureau of Meteorology for access to radio-sonde measurements.

References and Notes

Andreae, M.O., and P. Merlet, Emission of trace gases and aerosols from biomass burning, *Global Biogeochemical Cycles*, *15* (4), 955 - 966, 2001.

Crutzen, P.J., and M.O. Andreae, Biomass burning in the tropics: Impact on atmospheric chemistry and biogeochemical cycles, *Science*, *250* (1669), 1990.

Delmas, R.A., A. Druilhet, B. Cros, P. Durand, C. Delon, J.P. Lacaux, J.M. Brustet, D. Serca, C. Affre, A. Guenther, J. Greenberg, W. Baugh, P. Harley, L. Klinger, P. Ginoux, G. Brasseur, P.R. Zimmerman, J.M. Grégoire, E. Janodet, A. Tournier, P. Perros, T. Marion, A. Gaudichet, H. Cachier, S. Ruellan, P. Masclet, S. Cautenet, D. Poulet, C. Bouka Biona, D. Nganga, J.P. Tathy, A. Minga, J. Loemba-Ndembi, and P. Ceccato, Experiment for Regional Sources and Sinks of Oxidants (EXPRESSO): An Overview, *Journal of Geophysical Research*, *104*, 30609- 30624, 1999.

Fishman, J., J.M. Hoell, R.D. Bendura, R.J. McNeil, and V.W.J.H. Kirchhoff, NASA GTE TRACE A Experiment (September - October 1992): Overview, *Journal of Geophysical Research*, *101*, 23865 - 23879, 1996.

Gonzalez, C.R., M. Schaap, G. de Leeuw, P.J.H. Builtjes, and M. van Loon, Spatial variation of aerosol properties over Europe derived from satellite observations and comparison with model calculations, *Atmospheric Chemistry & Physics*, *3*, 521–533, 2003.

Goode, J.G., R.J. Yokelson, D.E. Ward, R.A. Susott, R.E. Babbitt, M.A. Davies, and W.M. Hao, Measurements of excess O_3, CO_2, CO, CH_4, C_2H_4, C_2H_2, HCN, NO, NH_3, HCOOH, CH_3COOH, HCHO, and CH_3OH in 1997 Alaskan biomass burning plumes by airborne Fourier transform infrared spectroscopy (AFTIR), *Journal of Geophysical Research*, *105*, 22147-22166, 2000.

Griffith, D.W.T., N.B. Jones, and W.A. Matthews, Interhemispheric ratio and annual cycle of carbonyl sulfide (OCS) total column from ground-based solar FTIR spectra, *Journal of Geophysical Research*, *103* (D7), 8447-8454, 1998.

Hurst, D.F., D.W.T. Griffith, and G.D. Cook, Trace gas emissions from biomass burning in tropical Australian savannas, *Journal of Geophysical Research*, *99* (D8), 16,441 - 16,456, 1994a.

Hurst, D.F., D.W.T. Griffith, and G.D. Cook, Trace gas emissions from biomass burning in tropical Australian savannas, *Journal of Geophysical Research*, *99* (D8), 16441 - 16456, 1994b.

Kaufman, Y.J.P., and e. al, Smoke, Clouds and Radiation - Brazil (SCAR-B) experiment, *Journal of Geophysical Research*, *103*, 31,783 - 31,808, 1998.

Lacaux, J.P., J.M. Brustet, R. Delmas, J.C. Menaut, L. Abbadie, B. Bonsang, H. Cachier, J. Baudet, M.O. Andreae, and G. Helas, Biomass burning in the tropical savannas of Ivory Coast: An overview of the field experiment Fire OF Savannas (FOS/DECAFE '91), *Journal of Atmospheric Chemistry*, *22*, 195 - 216, 1995.

Lindesay, J.A., M.O. Andreae, J.G. Goldammer, G. Harris, H.J. Annegarn, M. Garstang, R.J. Scholes, and B.W. van Wilgen, International Geosphere-Biosphere Programme/International Global Atmosphreric Chemistry SAFARI 92 field experiment: Background and Overview, *Journal of Geophysical Research*, *101* (D19), 23521 - 23530, 1996.

Paton-Walsh, C., N. Jones, S. Wilson, A. Meier, N. Deutscher, D. Griffith, R. Mitchell, and S. Campbell, Trace gas emissions from biomass burning inferred from aerosol optical depth, *Geophysical Research Letters*, *31* (5), 2004.

Phillips, F., Determination of Atmospheric Ozone by Solar Infrared, Ultraviolet and Visible Spectroscopy, Ph.D. thesis, University of Wollongong, Wollongong, 2001.

Rinsland, C.P., N.B. Jones, B.J. Connor, J.A. Logan, A. Goldman, F.J. Murcray, T.M. Stephen, N.S. Pougatchev, R. Zander, P. Demoulin, and E. Mahieu, Northern and Southern Hemisphere Ground-Based Infrared Spectroscopic Measurements of Tropospheric Carbon Monoxide and Ethane, *Journal of Geophysical Research*, *103*, 28,197-28,218, 1998.

Rinsland, C.P., C. Paton-Walsh, A. Goldman, N.B. Jones, D.W.T. Griffith, S.W. Wood, L.S. Chiou, and A. Meier, High Spectral Resolution Solar Absorption Measurements of Ethylene (C2H4) in a Forest Fire Smoke Plume using HITRAN 2000 Parameters: Tropospheric Vertical Profile Retrieval, *J. Quant. Spectrosc. Radiat. Transfer*, *96*, 301-309, 2005.

Rodgers, C.D., *INVERSE METHODS FOR ATMOSPHERIC SOUNDING: Theory and Practice*, 256 pp., World Scientific Books, 2000.

Shirai, T., D.R. Blake, S. Meinardi, F.S. Rowland, J. Russell-Smith, A. Edwards, Y. Kondo, M. Koike, K. Kita, T. Machida, N. Takegawa, N. Nishi, S. Kawakami, and T. Ogawa, Emission estimates of selected volatile organic compounds from tropical savanna burning in northern Australia, *Journal of Geophysical Research*, *108* (D3), 8406, 2003.

Swap, R.J., H.J. Annegarn, J.T. Suttles, M.D. King, S. Platnick, J.L. Privette, and R.J. Scholes, Africa burning: A thematic analysis of the Southern African Regional Science Initiative (SAFARI 2000). *Journal of Geophysical Research*, *108* (D13), 8465, 2003.

Torres, O., P.K. Bhartia, A. Sinyuk, E.J.W. and, and B. Holben, Total Ozone Mapping Spectrometer measurements of aerosol absorption from space: Comparison to SAFARI 2000 ground-based observations, *Journal of Geophysical Research*, *110* (D10S18), 2005.

Trentmann, J., M.O. Andreae, and H.-F. Graf, Chemical processes in a young biomass-burning plume, *Journal of Geophysical Research*, *108* (D22), 4705, 2003.
Wilson, S.R., and B.W. Forgan, Aerosol optical depth at Cape Grim, Tasmania, 1986 -1999, *Journal of Geophysical Research*, *107* (D8), 2002.

Figure Captions:

Figure 1: Vertical column amounts of CO, H_2CO, C_2H_6, HCN, C_2H_4, NH_3, HCOOH and C_2H_2 derived from individual spectra, plotted against simultaneous, co-located measurements of AOD. The data have been colour-coded to distinguish different time periods. The error-bars are the total uncertainty in the derived column amount for each spectrum and the one-sigma standard deviation of the aerosol optical depth measurements during the time taken to record each infrared spectrum.

Table 1: shows the spectral interval or intervals used for the retrieval of each trace gas, the interfering gases that were also fitted in the retrieval, and the mean values of the main uncertainties (1σ) affecting the precision of these retrievals.

Trace Gas	Spectral Interval(s) fitted	Interfering Gases Fitted in retrieval	Smoothing Uncertainty	Signal-to-noise Uncertainty	Temperature Uncertainty	Total Uncertainty
C_2H_4	945.00 – 952.00	H_2O, CO_2, NH_3	3.5%	3.8%	3%	6.4%
NH_3	1046 – 1046.75	H_2O, O_3, CH_4	14.5%	16.5%	2.7%	22.4%
HCOOH	1104.40 – 1106.00	H_2O, HDO, O_3	5.8%	26.6%	2.0%	27.5%
CO	2057.68 – 2058.00 2069.55 – 2069.76	CO_2, O_3	5.8%	2.5%	1.3%	6.5%
H_2CO	2778.12 – 2778.80 2780.60 – 2781.17	CO_2, O_3, CH_4	3.1%	10.8%	1.6%	11.4%
C_2H_6	2976.60 – 2977.10 2996.70 – 2997.10 3000.10- 3000.60	H_2O, H2CO, CH_4	4.4%	3.0%	2.3%	5.8%
C_2H_2	3304.80 – 3305.30	H_2O, HDO	4.7%	8.5%	1.9%	10%
HCN	3268.00 – 3268.38 3287.00 – 3287.48	H_2O	9.8%	3.3%	2.1%	10.6%

Table 2: shows the results of generalised least squares regression analysis on the column amounts of each trace gas and the coincident AOD measurements. The equations relating trace gas amounts and AOD are in the format: *Trace gas = "Slope"(AOD) + "Intercept"* and the Slope and Intercept for each gas is given along with the 1σ uncertainties from the regression analysis. It is important to note that the uncertainty in the regression analysis is an under-estimate of the true uncertainty because it assumes that the uncertainties are uncorrelated. Also there are significant other systematic uncertainties in the forward model that will contribute to the accuracy of these equations such as the uncertainties in the HITRAN 2000 line parameters used.

Trace Gas	Slope	Intercept
C_2H_4	$(9.8 \pm 0.8) \times 10^{15}$	$-(1.9 \pm 1.7) \times 10^{15}$
NH_3	$(8.2 \pm 0.4) \times 10^{15}$	$(2.4 \pm 0.2) \times 10^{15}$
HCOOH	$(2.1 \pm 0.1) \times 10^{16}$	$(0.1 \pm 0.1) \times 10^{16}$
CO	$(1.5 \pm 0.1) \times 10^{18}$	$(1.5 \pm 0.1) \times 10^{18}$
H_2CO	$(2.5 \pm 0.1) \times 10^{16}$	$(0.1 \pm 0.1) \times 10^{16}$
C_2H_6	$(3.4 \pm 0.1) \times 10^{15}$	$(7.2 \pm 0.1) \times 10^{15}$
C_2H_2	$(3.5 \pm 0.1) \times 10^{15}$	$(3.9 \pm 0.1) \times 10^{15}$
HCN	$(5.3 \pm 0.2) \times 10^{15}$	$(4.8 \pm 0.2) \times 10^{15}$

Table 3: Emission factors calculated in this study alongside the mean emission factor of each trace gas from extra-tropical forest measurements taken from [*Andreae*, 2005; *Andreae and Merlet*, 2001], including updates from M.O. Andreae, personal communication, M.O. Andreae, 2005. The uncertainties quoted for this study are derived from the large uncertainty in the emission factor for CO, (35%), combined in quadrature with the one-sigma standard deviation in the emission ratio to CO for each trace gas. The uncertainties shown for the mean emission factors from extra-tropical forest measurements are the one-sigma standard deviations of all the measurements used.

Trace Gas	No.of Spectra	Emission Ratio to CO (mol/mol)	Emission Factor (this study) g kg^{-1} (dry fuel)	Emission Factor (Andreae & Merlet) g kg^{-1} (dry fuel)
C_2H_4	77	0.0057 ± 0.0027	0.61 ± 0.36	1.2 ± 0.5
NH_3	68	0.0095 ± 0.0035	0.62 ± 0.31	1.7 ± 1.3
HCOOH	75	0.021 ± 0.010	3.7 ± 2.1	2.4 ± 2.3
H_2CO	60	0.023 ± 0.007	2.6 ± 1.2	1.9 ± 0.7
C_2H_6	79	0.0023 ± 0.0005	0.26 ± 0.11	0.73 ± 0.41
C_2H_2	77	0.0034 ± 0.0014	0.34 ± 0.18	0.26 ± 0.11
HCN	77	0.0042 ± 0.0016	0.43 ± 0.22	(0.81)

Figure 1: (a-d)

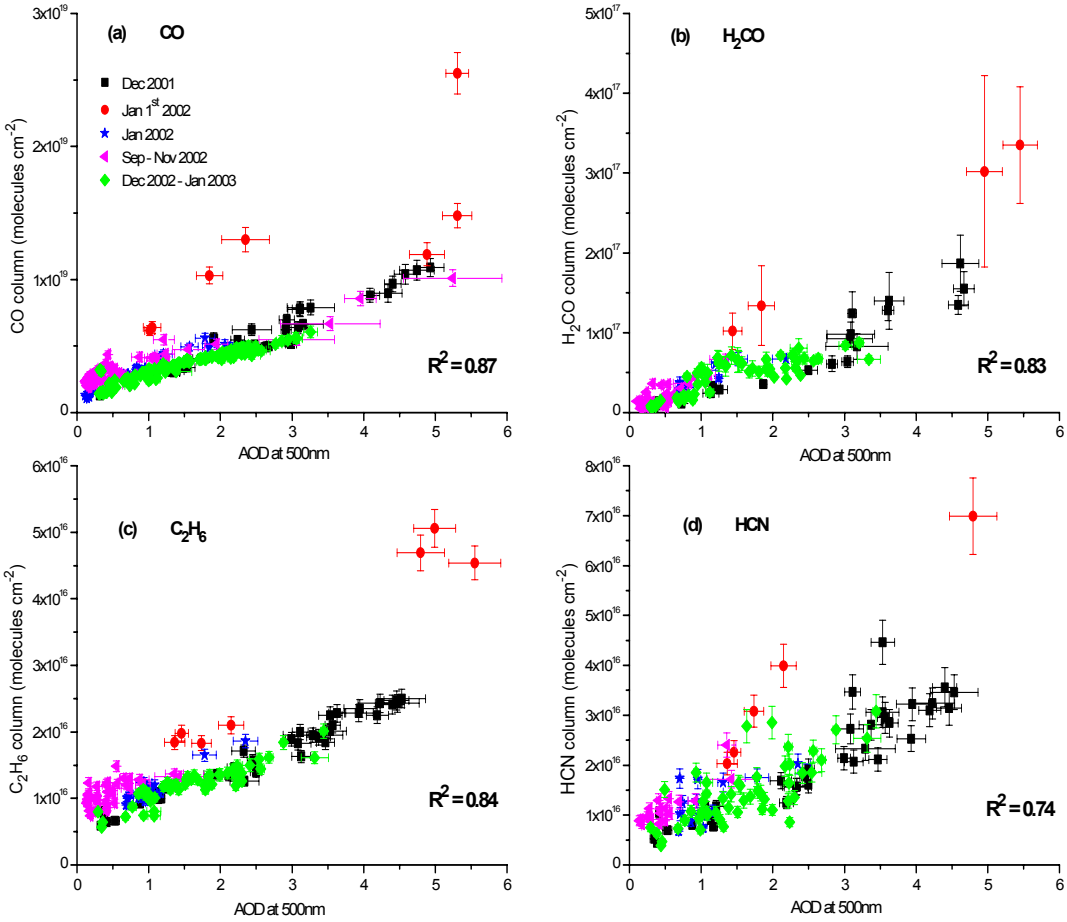
(a) CO
Dec 2001
Jan 1st 2002
Jan 2002
Sep - Nov 2002
Dec 2002 - Jan 2003
CO column (molecules cm-2)
R2 = 0.87
AOD at 500nm
(b) H2CO
H2CO column (molecules cm-2)
R2 = 0.83
AOD at 500nm
(c) C2H6
C2H6 column (molecules cm-2)
R2 = 0.84
AOD at 500nm
(d) HCN
HCN column (molecules cm-2)
R2 = 0.74
AOD at 500nm

Figure 1: (e-h)

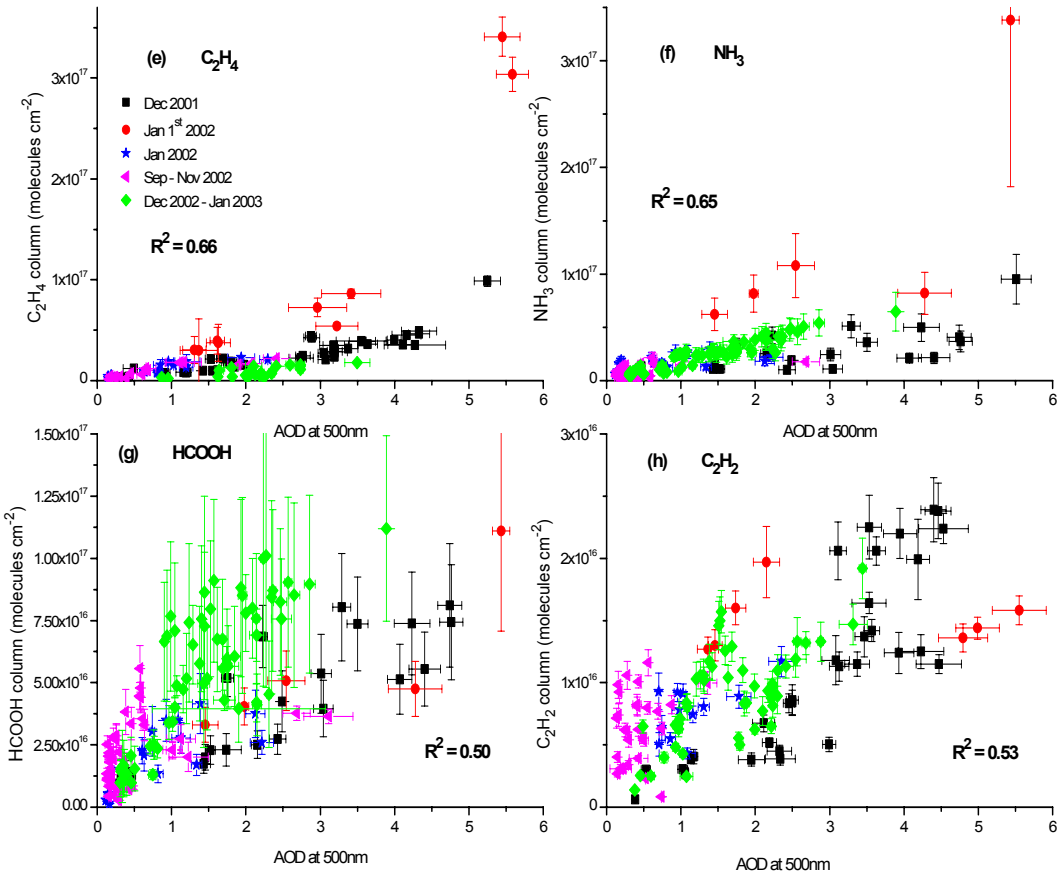
(e) C_2H_4
Dec 2001
Jan 1st 2002
Jan 2002
Sep - Nov 2002
Dec 2002 - Jan 2003
$R^2 = 0.66$
C_2H_4 column (molecules cm^{-2})
(f) NH_3
$R^2 = 0.65$
NH_3 column (molecules cm^{-2})
(g) HCOOH
$R^2 = 0.50$
HCOOH column (molecules cm^{-2})
(h) C_2H_2
$R^2 = 0.53$
C_2H_2 column (molecules cm^{-2})
AOD at 500nm